Compare Results

Old File:		New File:
GMD-Meyer-et_al.pdf	versus	**GMD-R1.pdf**
20 pages (1.47 MB)		**23 pages (2.37 MB)**
5/19/2022 8:26:43 AM		10/5/2022 11:30:19 AM

Total Changes

375

Text only comparison

Content

135 Replacements

141 Insertions

99 Deletions

Styling and Annotations

0 Styling

0 Annotations

Go to First Change (page 1)

Operational water forecast ability of the HRRR-iSnobal combination; an evaluation to adapt into production environments

Joachim Meyer[1], John Horel[2], Patrick Kormos[3], Andrew Hedrick[4], Ernesto Trujillo[5,4], S. McKenzie Skiles[1]

[1] Department of Geography, University of Utah, Salt Lake City, UT, USA
[2] Department of Atmospheric Sciences, University of Utah, Salt Lake City, UT, USA
[3] Colorado Basin River Forecast Center NOAA National Weather Service, Salt Lake City, UT, USA
[4] Northwest Watershed Research Center, USDA Agricultural Research Service, Boise, ID, USA
[5] Department of Geosciences, Boise State University, Boise, ID, USA

Correspondence to: Joachim Meyer (j.meyer@utah.edu)

Abstract

Operational water-resource forecasters, such as the Colorado Basin River Forecast Center (CBRFC) in the Western United States rely on historical records to calibrate the temperature-index models currently used for snowmelt runoff predictions. This data dependence is increasingly challenged, with global and regional climatological factors changing the seasonal snowpack dynamics in mountain watersheds. To evaluate and improve the CBRFC modeling options, this work ran the physically based snow energy balance iSnobal model, forced with outputs from the High-Resolution Rapid Refresh (HRRR) numerical weather prediction model across four years in a Colorado River Basin forecast region. Compared to in-situ, remotely sensed, and the current operational CBRFC model data, the HRRR-iSnobal combination showed well-reconstructed snow depth patterns and magnitudes until peak accumulation. Once snowmelt set in, HRRR-iSnobal showed that simulated snowmelt was slower relative to observations, depleting snow on average up to 34 days later. The melting period is a critical component for water forecasting. Based on the results, there is a need for revised forcing data input preparation (shortwave radiation) required by iSnobal, which is a recommended future improvement to the model. Nevertheless, the presented performance and architecture make HRRR-iSnobal a promising combination for the CBRFC production needs, where there is a demonstrated change to the seasonal snow in the mountain ranges around the Colorado River Basin. The long-term goal is to introduce the HRRR-iSnobal combination in day-to-day CBRFC operations, and this work created the foundation to expand and evaluate larger CBRFC domains.

1

1. Introduction

Freshwater supply, originating as melt from seasonal snowpack runoff, has experienced a shift in timing and magnitude in recent decades (Mote et al., 2018; Stewart, 2009). Higher observed temperatures during the winter (Musselman et al., 2021), for instance, lead to precipitation phase changes resulting in more precipitation as rain over snow in low elevation areas (Feng and Hu, 2007; Knowles et al., 2006). The magnitude of the changes varies regionally (Harpold et al., 2012; Skiles and Painter, 2017), which increases the complexity of understanding and forecasting the impacts. Changing snowpack trends are expected to continue, as evidenced by simulations with predicted future climate conditions (Cho et al., 2021; Ikeda et al., 2021; Li et al., 2017; Musselman et al., 2017). This presents a challenge from a modeling perspective, especially in operational settings, when historical data are the basis to create forecasts. Here, a consistent and accurate prediction of snowpack runoff is getting harder with the increasingly different snow accumulation, snow melt, and snow cover extents across the seasonally snow-covered mountain ranges supplying freshwater to the downstream regions.

Presently, a subset of the hydrologic forecast agencies in the United States use temperature-index models, such as SNOW-17 (Anderson 1976), which have historically performed well in operational settings while requiring few meteorological observations (Franz et al., 2008). In principle, SNOW-17 calculates the snowmelt using the correlation between air temperature and available melt energy from net solar radiation and a calibration factor, which increases as the melt period progresses (Anderson, 1976; Franz et al., 2010). The best model predictions are with domain-specific calibration parameters from historical data with the modeled year following the snow accumulation and melt conditions from the past (He et al., 2011). Once conditions depart from the historical average, such as lower snow albedo from highly variable inter-annual dust deposition events (Bryant et al., 2013), the SNOW-17 model forecast errors increase and require significant forecaster interaction to account for the variable conditions. One effort to improve the accuracy of SNOW-17 applied the Bayesian Model Averaging method across an ensemble of twelve snow models, each consisting of different components from SNOW-17 (Franz et al., 2010). Although the results improved compared to running SNOW-17 as a standalone application, the setup was only tested at the 1d point scale and required different weights for the individual models between test locations. This increased complexity makes the method challenging to apply across larger spatial scales in daily operations. Ultimately, temperature-index models cannot adapt to rapidly changing snow accumulation and melt conditions and the long-term historical records (30 to 40 years) are becoming less representative to calibrate the model parameters.

One option to improve forecasting results is the use of physically based models that incorporate more meteorological measurements and are not calibrated on historical observation data. Physically based modeling is also referred to as 'energy-balance' or 'process-based' in the literature, and in the context of this work, we will use 'physically based'. In general, physically based models use additional weather observations outside of temperature and precipitation such as relative humidity, wind speeds, and radiation, to resolve the mass and energy balances of the snowpack, which determines the snowmelt rate and meltwater runoff (Marks and Dozier, 1992). From the several physically based snow model options developed to date (e.g., CROCUS, Vionnet et al., 2012; Factorial Snow Model, Essery, 2015; SNOWPACK, Lehning et al., 2002; SnowModel, Liston and Elder, 2006), this work focused on iSnobal. Initially, iSnobal was implemented as a two-layer snowpack model for a single point location (Marks and Dozier, 1992; Marks et al., 1992) and evolved later to a spatially distributed version (Marks et al., 1999), maintaining the design and input data requirements of the point-level version. A recent addition to the iSnobal modeling pipeline is the Spatial Modeling for Resource Framework (SMRF, Havens et al., 2017), which assists in distributing the forcing data across the model domain. To streamline the iSnobal data preparation and execution workflow and increase reproducibility, the Automated Water Supply Model (AWSM) combined iSnobal and SMRF into a single modelling framework (Havens et al., 2020). To this date, iSnobal has been

successfully deployed to simulate snowpacks in watersheds sizes from less than 1 km² to over 1000 km² (Garen and Marks, 2005;
Hedrick et al., 2018, 2020; Kormos et al., 2014).

The increased meteorological measurement requirements to calculate the mass and energy balances of physically based models cannot always be satisfied by in-situ observation networks. Where instrumentation sites are present in the modeled domain, the available observations are not guaranteed to provide all required model inputs such as wind speed or radiation, can have data gaps through time, or do not satisfy the necessary data quality. An alternative to in-situ stations is using outputs from numerical weather prediction (NWP) models, which are generally spatially and temporally complete and provide all the required forcing variables from a single source. The adaptation of NWP model output to provide forcing data for snow models is ongoing and has been successfully tested as a standalone source for point simulations (Bellaire et al., 2011, 2013; Iwamoto et al., 2008) or spatially in combination with data assimilation and filtering techniques (Griessinger et al., 2019; Vernay et al., 2021). Adding NWP as a possible weather measurement input source to iSnobal was first evaluated in Havens et al. (2019), where downscaled and bias-corrected observations from Weather Research and Forecasting (WRF) Model had the best results. A follow-up effort to the WRF integration into iSnobal also added support for the High-Resolution Rapid Refresh (HRRR) model (Benjamin et al., 2016) from the National Oceanic and Atmospheric Administration (NOAA). HRRR assimilates available real-time observations every hour and produces forecasts up to 18-hours in advance. The HRRR product outputs are delivered at the 3 km spatial resolution for the continental United States and the Alaska domain. The HRRR model has been under active development since it became the United States National Weather Service's (NWS) operational forecast model in late 2014 (Bytheway et al., 2017) and is currently in its fourth and final iteration. The HRRR data are publicly via different providers (Google Cloud Platform, Amazon Web Services, NOAA) and are readily integrable for research and operational purposes (Gowan et al., 2022).

Among the many regions impacted by the changing seasonal snow and environmental conditions around the globe (Ayers et al., 2016; Cho et al., 2021; Christensen and Lettenmaier, 2007; Dettinger et al., 2015) is the Western United States of America, where 53% to 70% of the annual freshwater supply originates from seasonal snowmelt (Li et al., 2017). For example, the Colorado River Basin (CRB), with its headwaters located in the Rocky Mountains, is currently trending towards a shorter duration and reduced extent of snow cover in the winter based on in-situ measurements from 1984 to 2009 (Harpold et al., 2012) and earlier dates for maximum snow water equivalent (SWE) compared to long-term historical records (Musselman et al., 2021). The CRB region also has an increase in snow darkening following the deposition of light-absorbing particles (Skiles and Painter, 2017; Skiles et al., 2012), which accelerates snowmelt timing and magnitude (Painter et al., 2018). Freshwater supply forecasting in this region is done by the Colorado Basin River Forecast Center (CBRFC), part of the National Weather Service (NWS) in the United States of America. The CBRFC uses SNOW-17 as part of their operational water availability forecasting model and faces increased challenges in adapting to the observed and predicted seasonal snow changes. The underlying long-term historical calibration records from the CBRFC do not fully account for climate variability and will continue to be less representative in the future. Capturing the different timing and magnitudes of snowmelt requires new methods.

In this paper, the HRRR-iSnobal combination is documented and described for the first time and assessed across four water years (2018 – 2021) in the East River Watershed, Colorado, USA. The model evaluation was in collaboration with the CBRFC to gauge the feasibility of supplementing SNOW-17 with a physically based model. A recent report by the United States Bureau of Reclamation evaluated iSnobal as a "flight qualified" product and supports the increased use of physically based models (The Bureau of Reclamation, 2022). In contrast to the current literature evaluating iSnobal in operational settings, this work focuses on HRRR as a standalone forcing input source without bias corrections (Havens et al., 2019) or updates from spatial observations (Hedrick et al., 2018, 2020). Removing input data corrections or model updates through in-situ observations increases the CBRFC's ability to adapt the workflow into their daily operations and speeds up model preparation and execution times. For the overall

iSnobal model assessment, the simulated snow depth was compared against measured observations at discrete in-situ snow measurement stations and spatially at discrete points in time against aerial snow depth maps. The iSnobal simulated runoff was compared to the basin hydrograph for basin-averaged assessment. Finally, HRRR-iSnobal precipitation inputs and SWE outputs were compared to SNOW-17 to assess the differences between the models. This work is an effort to support the increased inclusion of physically based models in operational water supply forecasting in snow-dominated environments. Broadly, this work also contributes to the NWS Advanced Hydrologic Prediction Service program operational goals (Council, 2006) by aiming to make hydrological forecasting more accurate and resilient in the face of change.

2. Study Area

The East River Watershed (ERW) is a high alpine watershed located in the Upper Gunnison River Basin, part of the Colorado River Basin. The East River is one of two primary tributaries of the Gunnison River, which discharges downstream into the Colorado River (Figure 1). A stream gauge station at an elevation of 2440 m near Almont, CO is operated by the United States Geological Survey (USGS) and monitors the streamflow of the East River year-round. This station is the central discharge point for seasonal snow runoff in the watershed. The ERW has representative characteristics for mountain watersheds in Colorado with an average elevation of 3266 m, high vertical elevation relief (1420 m; Hubbard et al., 2018), and a mixture of different vegetation types (bush and grassland or mixed conifer and aspen trees).

There are three Snow Telemetry (SNOTEL) stations with available snow depth measurements that are operated by the United States Department of Agriculture National Resource Conservation Service (USDA-NRCS) in the modeled domain: Schofield Pass (SP hereafter; elevation: 3261 m), Butte (elevation: 3097 m), and Upper Taylor (UT hereafter; elevation: 3243 m). The Upper Taylor station does not sit within the ERW boundaries but was included in this study to expand the number of available in-situ comparison sites within the model domain. The CBRFC divides the ERW into three topographical hydrologic response units (HRU); lower, middle, and upper (Figure 1). Each HRU is based on elevation (2896 m/9500 ft < middle < 3353 m/11000 ft) and
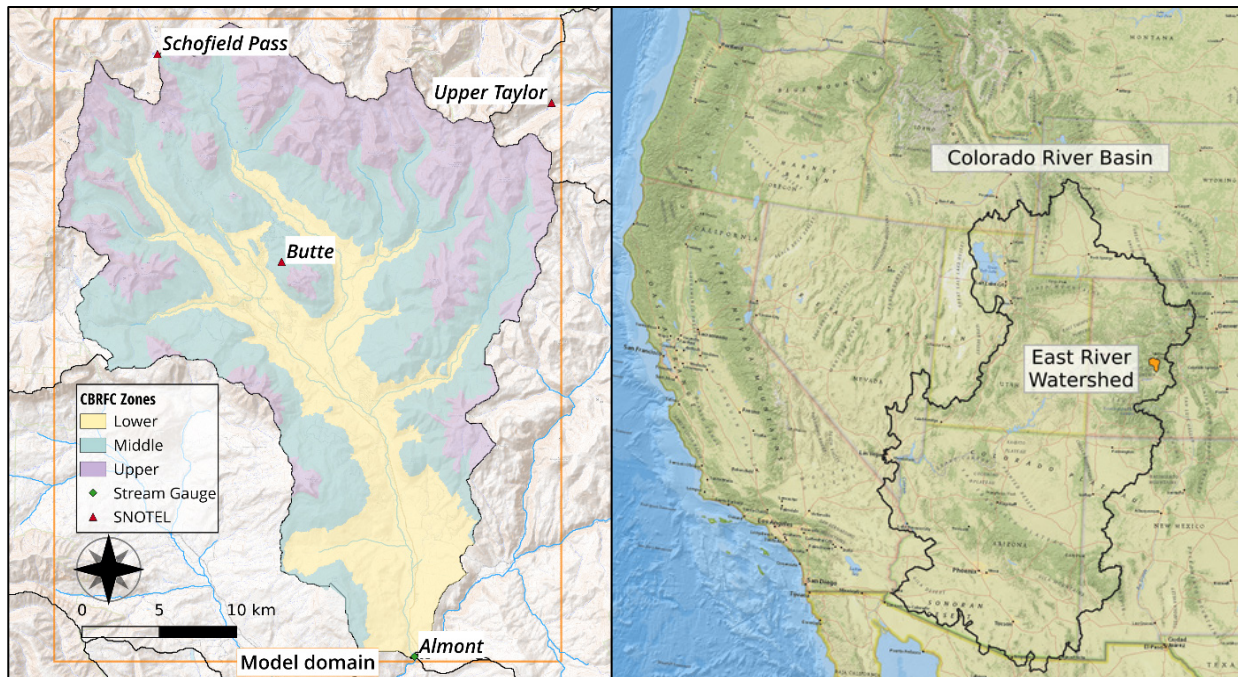

Figure 1 – Overview of the East River Watershed (black boundaries) and iSnobal modal domain (orange outline) are shown on the left. There are three SNOTEL sites along with the stream gauge station. The watershed is divided into three HRUs by the CBRFC. The location of the watershed and area of the Colorado River Basin is shown on the right. Basemap (right): © ESRI

125 are modeled independent from each other (Council, 2006). The division will be used in this work to refer to the respected spatial area.

3. Model

3.1 Model Architecture

A complete setup of the iSnobal model requires the installation of several
130 components (Figure 2). First, the 'Basin Setup' tool (https://github.com/USDA-ARS-NWRC/basin_setup) is installed, which assists in setting up the model domain boundaries, output resolution, and collecting the elevation and vegetation data. This one-time process is not repeated between simulation years and stored in one central basin metadata file. Next, the daily execution components of the model are set up
135 and consist of:

- Katana (https://github.com/USDA-ARS-NWRC/katana)
- SMRF (https://github.com/USDA-ARS-NWRC/smrf)
- AWSM (https://github.com/USDA-ARS-NWRC/awsm)

Katana is a pre-processing module that uses the WindNinja model (Forthofer et al.,
140 2014) at its core to downscale the HRRR wind data to a higher resolution (e.g., from HRRR 3 km to 200 m). The SMRF module (Havens et al., 2017) develops the high resolution hourly spatial forcing data required by iSnobal using coarser resolution HRRR surface variables. AWSM (Havens et al., 2020) is the overarching control software that streamlines the execution for each time step and the iteration from one to the next day between SMRF and iSnobal.
145 All the above components were written and are maintained by the United States Department of Agriculture, Agriculture Research Service (USDA-ARS) in Boise, ID, USA. Each component is fully open-source software and installable from source via GitHub (https://github.com) or downloadable as a Docker container. A Docker container is a virtualized environment that combines the required operating system, libraries, and the application itself into one executable entity.

Figure 2 - Overview of the iSnobal model architecture showing the one-time set process and the daily execution workflow.

3.2 East River Watershed Model Domain Setup and Execution

150 Elevation data at 1/3 arcsecond (approximately 10-m) resolution from the United States Geological Survey (USGS) National Elevation Dataset and 30-m vegetation data (height and type) from the USGS through the LANDFIRE spatial products were used as input for the Basin Setup tool. Both data sources are publicly available and distributed through the USGS (see Data availability section). Basin Setup was further configured to prepare the ERW model domain at a 50 m spatial resolution, resulting in 837 x 656 grid cells and an area of 1373 km². This spatial resolution was guided by the recommendations of Winstral et al. (2014), which
155 found that iSnobal output resolutions of around 100 m kept the errors for SWE and SWI below +/-5% during melt season compared to coarser resolutions. We further selected the 50 m resolution to keep the resampling of the vegetation data from LANDFIRE minimal and removed the need to interpolate the spatial snow depth product used in validation (section 4 Model Comparison). This resolution additionally better represents the terrain complexity, relevant for radiation calculations and interpolation of the HRRR supplied forcing data within SMRF. Lastly, we also found that the 50 m resolution does not inhibit daily run times and
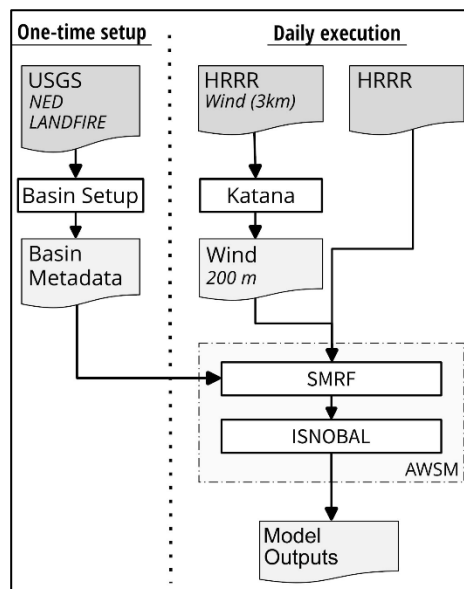160 scales for the operational requirements.

Snowpack mass and energy fluxes were simulated with iSnobal from 2018 through 2021 in one-hour time steps, matching the HRRR temporal resolution. The model was configured to store the end-of-day values (e.g. snow depth) or accumulated daily values (e. g. SWI), matching the temporal resolution of the available in-situ comparison observations and the SNOW-17 inputs and outputs, which are further explained in the model comparison section. A single simulation year starts on the 1st of October and ends on the 30th of September. This date range is a 'water year' and a standard definition for hydrologic forecasting in the United States.

3.3 Model Forcing Data

The meteorological inputs required to run the model were retrieved from the sixth-hour HRRR forecast product. HRRR is undergoing active development, and the water years simulated in this study used the product versions HRRRv2 (October 2017 to July 2018), HRRRv3 (July 2018 to November 2020), and HRRRv4 (December 2020 to August 2021). Using the sixth-hour HRRR forecast allows for better utilization of model physics along with the assimilated observations (Bytheway et al., 2017) and is a common practice for other NWP input products (Schirmer and Jamieson, 2015).

The required iSnobal forcing input data supplied from HRRR are: air temperature, relative humidity, incoming shortwave radiation, wind speed and direction, and total precipitation. Using the wind data from HRRR (U and V component, 10 m above ground), Katana resolves the wind data to a 200 m resolution using the model domain elevation data. The 200 m resolution was a compromise between the iSnobal simulated resolution (50 m) and the increased computational resources required by WindNinja to downscale from the 3 km HRRR grid.

3.4 iSnobal and SMRF Description

Using temporally complete meteorological input data, the iSnobal model (Marks et al., 1999) simulates snowpack evolution by solving energy and mass balance fluxes. As a two-layer model, the top layer is designated for all energy and mass exchanges between the snow surface and the atmosphere. The bottom layer acts as an interface for mass and energy exchanges between the top and a single soil layer. At each simulated time step (1 hour for the current application), the model calculates the snowpack net radiative, sensible, latent, conductive, and advective energy fluxes. Once the net energy fluxes of the two snow layers exceed the cold content (the energy required to raise the temperature across both layers to 0 °C) and the snow meltwater amount exceeds the maximum liquid water holding capacity of the snowpack, the water outflow at the base of the snowpack is calculated (i.e., surface water input (SWI) hereinafter). At the end of a time step, the updated snowpack state variables (depth, density, temperature, and liquid water content) are stored and used as initialization values at the beginning of the next time step.

Before calculating the fluxes, the input data are spatially interpolated and distributed for the model domain in SMRF, which also prepares additional essential variables for the energy balance calculations in iSnobal. The variables include information for precipitation phase, precipitation temperature, percentage of snow in precipitation, and water vapor pressure. The required net shortwave radiation input used in iSnobal is calculated by SMRF from the topographically adjusted incoming clear sky radiation (Dozier and Frew, 1990) and reduced with the percentage of cloud cover. The cloud cover itself is determined by the supplied incoming shortwave radiation from HRRR. An additional adjustment to the incident shortwave radiation reduces the value by vegetation type and height information from the vegetation metadata following Link and Marks (1999). The amount of reflected shortwave radiation is calculated using a simulated snow albedo derived with a time-decay function based on the time duration since last snowfall. The difference between the cloud and vegetation-adjusted incident shortwave and the reflected shortwave results in the net shortwave radiation at the snow surface.

The net longwave radiation is calculated similar to the net shortwave radiation in SMRF. First, the percentage of cloud cover is used to adjust the incoming longwave fluxes from a theoretical clear-sky atmosphere before the vegetation data is used to do a final correction (Link and Marks, 1999). From the downscaled wind data from the Katana module, SMRF interpolates the wind speeds to the configured output resolution. The SMRF options include the ability to account for precipitation redistribution using the speed and direction wind data according to Winstral et al. (2002). However, this option was not used in this study and reduced potential error sources when comparing the HRRR precipitation input data to Snow-17, which is explained in section 4 below.

A detailed description of the energy balance equations and data preparation can be found in Marks et al. (1992), Marks et al. (1998, 1999), Link and Marks (1999), and Havens et al. (2017; 2020). All energy and mass balance calculations in iSnobal are based on a fixed spatial grid and a configurable time interval. The main driver for the chosen time interval to update the snowpack conditions is the temporal resolution of the input data, which needs to be fine enough to resolve diurnal climatic variations (e.g., temperature or shortwave radiation).

3.5 Model Computing Environment

The computational resources required for running the model in this work were provided by the Center for High Performance Computing at the University of Utah. All model components were installed from source, with the exception for Katana, where the containerized option was selected due to the complexity of dependent libraries. The installation was documented and published on GitHub (https://github.com/UofU-Cryosphere/isnoda) and extends the official documentation for each component with instructions for a shared compute environment and helper scripts for data download and model execution.

4 Model Comparison

Two types of measurements were used to compare selected iSnobal outputs with reference values: discrete in-situ time-series measurements and spatially distributed snapshots at a single point in time. The in-situ observations were the quality-controlled end-of-day values for snow depth measurements from the three SNOTEL stations. This assessment against the SNOTEL data used a spatial maximum and minimum of a 2x2 grid surrounding the point location of the sites (Figure 3). This approach was based on visual inspections of the locations. Each site showed an offset to the center of the model output cell, and a spatial grid was deemed more appropriate to account for the physiographic variability surrounding their location. For the years with available Airborne Snow Observatory (ASO, Painter, et al., 2016) spatial observations (2018 to 2020), simulated snow depths were compared to the ASO lidar snow depths. The range of snow depth values on ASO flight days was also included in the time-series comparison and used the same 2x2 grid surrounding the SNOTEL sites (Figure 3).

The spatial point in time comparison used lidar-based snow depth maps from ASO, which surveyed the area twice in 2018 and 2019 and once in 2020. In 2018 and 2019, the first survey happened during the snow accumulation season, and the second survey happened after peak SWE during snowmelt progression. In 2020, the area was surveyed before peak SWE. The spatial resolution of the ASO snow depth maps matched the iSnobal model resolution of 50 m, and the spatial extent overlapped with the ERW boundaries. Across the years, the ASO snow depth maps were used as the reference, and the model simulated snow depth was subtracted from the lidar snow depth on a pixel-by-
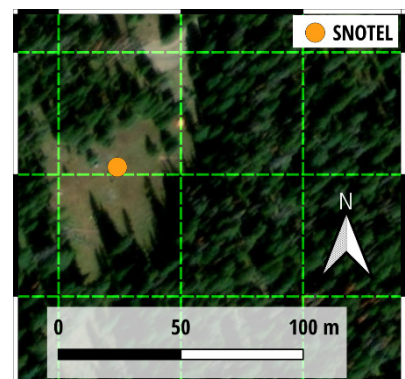

Figure 3 – SNOTEL Schofield Pass site location relative to configured model output resolution of 50 m (green dashed grid). No site was centered in one pixel and a spatial 2x2 grid surrounding the site was used for simulated **HRRR-iSnobal** comparison values. Basemap: © ESRI

pixel basis. The goal of this comparison was to check for any spatial biases in simulated snow depths across elevation bands or aspects and for different snow conditions (accumulating or melting) in years with two flights (2018 and 2019).

To assess how well the iSnobal simulated melt aligned with the ERW snowmelt-dominated hydrograph, all SWI of the model grid cells in the watershed boundaries were summed up and compared against the stream gauge at the basin pour point. This comparison used a seven-day moving average window to reduce daily spikes in the time series. The focus of this evaluation was on timing and magnitude; in a basin like ERW, the simulated SWI should follow the temporal pattern measured at the stream gauge, which is influenced by the snowmelt runoff. Finally, to better understand how HRRR-iSnobal compares to SNOW-17 for operational forecasting, the precipitation inputs and SWE outputs from both models were compared. The gridded iSnobal data was summarized by HRU (Figure 1) and individually compared to the SNOW-17 input/output data provided by the CBRFC. Mean areal precipitation values by the CBRFC originate from precipitation measurement stations in and around ERW, are quality controlled, and combined using a weighting equation derived during calibration with the primary target being PRISM (Parameter elevation Regression on Independent Slopes Model) statistical mapping grids. Neither of these datasets are considered the true values; rather, this model inter-comparison was undertaken to understand how (and why) the models may differ. Additionally, iSnobal simulated snow depths were compared to ASO lidar snow depths in each HRU.

5. Results

5.1 Run time

Running the model through an entire water year took around eighteen hours in total, with WindNinja taking one-third of the time, and AWSM accounting for the remaining 12 hours. The compute times are based on a machine with 24 processor cores, 24 GBs of RAM, and hyper-threading enabled, which increased the number of processing threads to 48. The storage requirement for the input data was 10 GBs, with the model output occupying another 100 GBs of space. Iterating from one day to the next took less than five minutes, including data download, pre-processing, and running the model. This reasonably fast execution and total storage requirement showed that the model could be implemented in day-to-day operations.

5.2 Point comparison

For the two sites within the ERW boundaries (Butte and SP), the simulated depths prior to peak snow depth had a mean difference of 12 % (0.05 m; Butte) and 1 % (0.01 m; SP) in 2018, -2 % (-0.01 m; Butte) and -15 % (-0.18 m; SP) in 2019, - 16 % (-0.09 m; Butte) and -21 % (-0.21 m; SP) in 2020, and -4 % (-0.02 m; Butte) and -3 % (0.03 m; SP) in 2021 until peak SWE (Supplement Figure S2). The UT site had consistently higher than observed snow depth: 37 % (0.27 m) in 2018, 23 % (0.22 m) in 2019, 28 % (0.22 m) in 2020, and 20 % (0.14 m) in 2021. (Supplement Figure S2). This site-specific result was consistent across all comparison years and not affected by annual differences in the accumulation magnitudes. Examples for an average snow depth year (2018) and an above-average year (2019) are shown in Figure 4. Results for 2020 and 2021 are shown in the Supplement Figure S1.

After the seasonal peak snow depth, simulated snow depths around all three SNOTEL stations deviated from observations and the range of simulated values increased. Notably, the date for snow disappearance was simulated later relative to observations across all years and varying difference of days. For instance, the difference between HRRR-iSnobal and all SNOTEL sites was between 11 to 59 days in 2018 and -8 to 59 days in 2019. An overview of the differences between observations and simulations dates is shown in Table 1. Consequently, the percentage mean difference between HRRR-iSnobal and SNOTEL snow depths increased considerably and values at the Butte site were 27 % (0.11 m) in 2018, 13 % (0.11 m) in 2019, -6 % (-0.04 m) in 2020, and 25 %
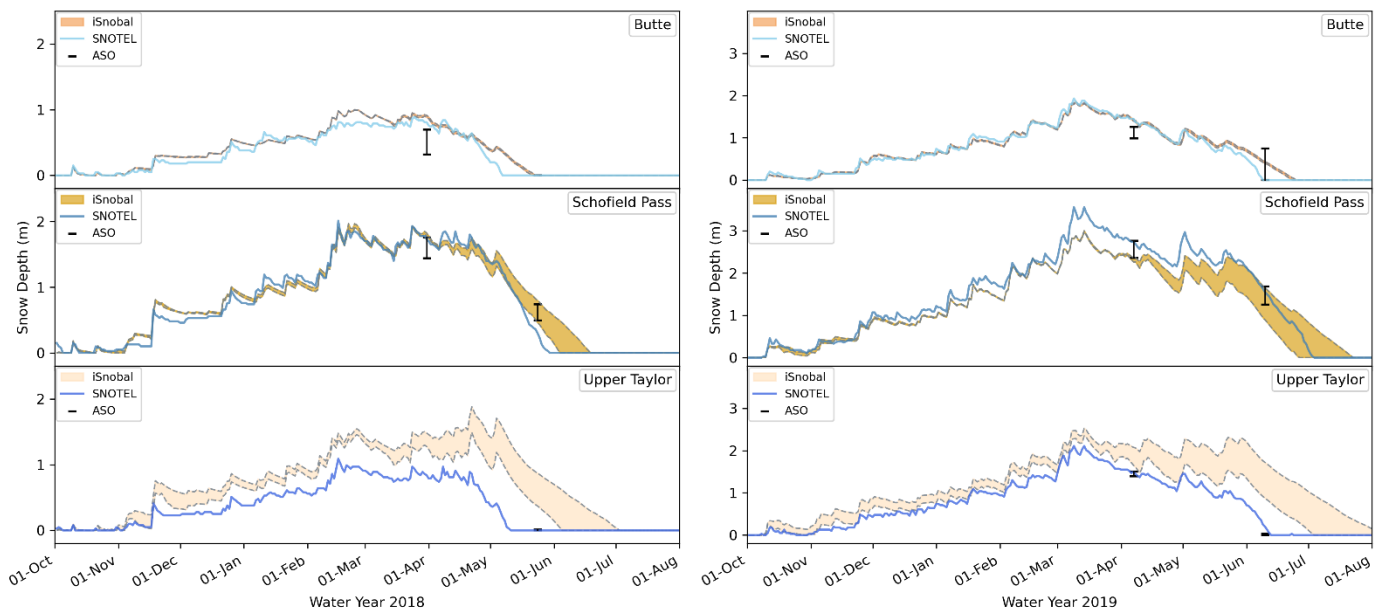
Figure 4 – Snow Depth comparison between iSnobal and SNOTEL sites for the years 2018 (left) and 2019 (right). The orange shaded areas represent the range of 2x2 grid cell values from iSnobal surrounding the site. The ranges of the grid cell (50 m) values from ASO surveys are shown by the black bars. Note the difference y-scales between 2018 and 2019.

(0.13 m) in 2021. The SP site mean differences were 19 % (0.15 m) in 2018, -17 % (-0.23 m) in 2019, -46 % (-0.27 m) in 2020. And -5 % (-0.04. m) in 2021. This disagreement in snowmelt rates and snow disappearance is further discussed in Section 6.4. Overall, the snow depth comparison to observations over multiple years showed that the model can capture peak snow depth timing and magnitude.

275   A cross-comparison of snow depths on ASO flight days between the observed in-situ SNOTEL sites, ASO remotely sensed, and HRRR-iSnobal simulated values showed a mixed result for agreement. The early season ASO flight in 2018 had HRRR-iSnobal with higher snow depths around the Butte (Mean difference (MD) +0.35 m) and SP (MD +0.20 m) sites compared to ASO. The difference between HRRR-iSnobal and SNOTEL were small, with the Butte site ranging from +0.10 m to +0.13 m and the SP site from +0.04 m to +0.08m. The late-season flight, where snow was only present at the SP site, had the HRRR-iSnobal snow depths

280   closer to ASO (MD -0.07 m) and above the SNOTEL values (+0.20 m to +0.54 m). The UT site was not included in both ASO surveys in 2018. For 2019, the early season ASO to HRRR-iSnobal snow depth differences varied with higher HRRR-iSnobal values at Butte (MD +0.25 m) and UT (MD +0.39 m) and lower values at SP (MD -0.22 m). The HRRR-iSnobal to SNOTEL differences were low at Butte (0.00 m to 0.04 m), negative at SP (-0.32 m to -0.43 m), and positive at UT (+0.16 m to +0.61 m). The late-season flight in 2019 had ASO higher than HRRR-iSnobal at Butte (MD +0.19 m) with no snow measured by SNOTEL,

Table 1 – Overview of date differences for last day with snow present between HRRR-iSnobal and SNOTEL sites.

SNOTEL site	**Melt dates**	**2018**	**2019**	**2020**	**2021**
	SNOTEL	05/06	06/08	05/12	05/12
Butte	*HRRR-iSnobal*	05/24 to 05/25	06/24 to 06/26	05/26 to 05/28	05/31 to 06/02
	Difference	18 – 19 days	16 – 18 days	14 – 16 days	19 – 21 days
	SNOTEL	05/29	07/03	06/03	06/02
Schofield Pass	*HRRR-iSnobal*	06/09 to 06/23	06/25 to 07/25	05/29 to 06/17	06/05 to 06/20
	Difference	11 – 25 days	-8 – 22 days	-5 – 14 days	3 – 18 days
	SNOTEL	05/10	06/12	05/13	05/13
Upper Taylor	*HRRR-iSnobal*	06/10 to 07/08	07/03 to 08/10	05/31 to 07/05	06/06 to 07/05
	Difference	31 – 59 days	21 – 59 days	18 – 53 days	24 – 53 days

9

while SP had HRRR-iSnobal lower than ASO (MD -0.31 m) and an overlapping range with SNOTEL measured (+0.11 m to -0.66 m). The UT site had HRRR-iSnobal much higher snow depths than ASO (MD +1.25 m) and SNOTEL (+0.71 m to +1.55 m). Overall, using ASO as an additional snow depth reference data set at discrete point locations in the model domain showed no consistent over or under-simulation for HRRR-iSnobal.

5.3 Spatial comparison

Integrated over the full basin, simulated snow depths agreed with ASO lidar snow depths, with a median difference of 0.20 m (early survey) and 0.00 m (late survey) in 2018, -0.06 m (early) and 0.00 m (late) in 2019, and 0.06 m in 2020. The distribution of the differences is shown with the 'All' category in Figure 5. Generally, between two flights in the same season, the agreement was best during late flights in the middle and lower HRU (Figure 5a and 5b). An aerial overview with per grid cell difference for the 2018 and 2019 flight is shown in Figure 6 and 2020 can be found in the Supplement Figure S3. Within lower, middle, and upper HRU elevations, the widest range in the Δ snow depth distribution was consistently found at the upper HRU (Standard Deviation 0.53 m in 2018; 0.89 m to 0.99 m in 2019; 0.55 m in 2022), while the narrowest range was found at the lower HRU (Standard Deviation 0.03 m to 0.17 m in 2018; 0.11 m to 0.55 m in 2019; 0.27 m in 2020). The middle HRU was in between (Standard Deviation 0.22 to 0.28 m in 2018; 0.48 m to 0.53 m in 2019; 0.30 m in 2020). The distributions of Δ snow depth for the late survey in each year showed positive biases, indicating a general overestimation of snow depths by HRRR-iSnobal, consistent with the observed slower snow depth decrease during the snowmelt season at the SNOTEL sites (Figure 4).

The snow depth differences binned by aspect for the entire watershed indicated a bias, with variation during flight dates and the two years (Figure 7a and 7b). In both early flights, higher snow depth was measured on eastern aspects relative to other aspects, and the widest ranges in snow depth differences were on northern aspects in both late flights. The closest agreement between modeled and ASO lidar snow depths was on south-facing slopes during late flights.
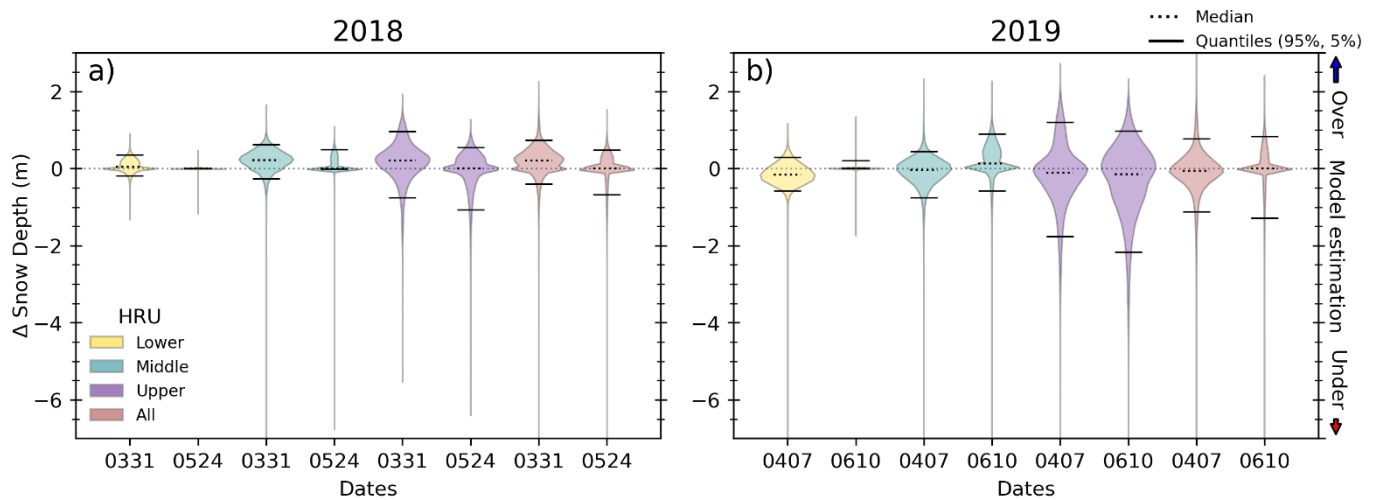

Figure 5 – Snow Depth Differences for early and late surveys for the years 2018 and 2019 between ASO and HRRR-iSnobal. Figure a) and b) categorize the differences by elevation HRU (low, middle, upper) with the 'All' showing the basin-wide difference.
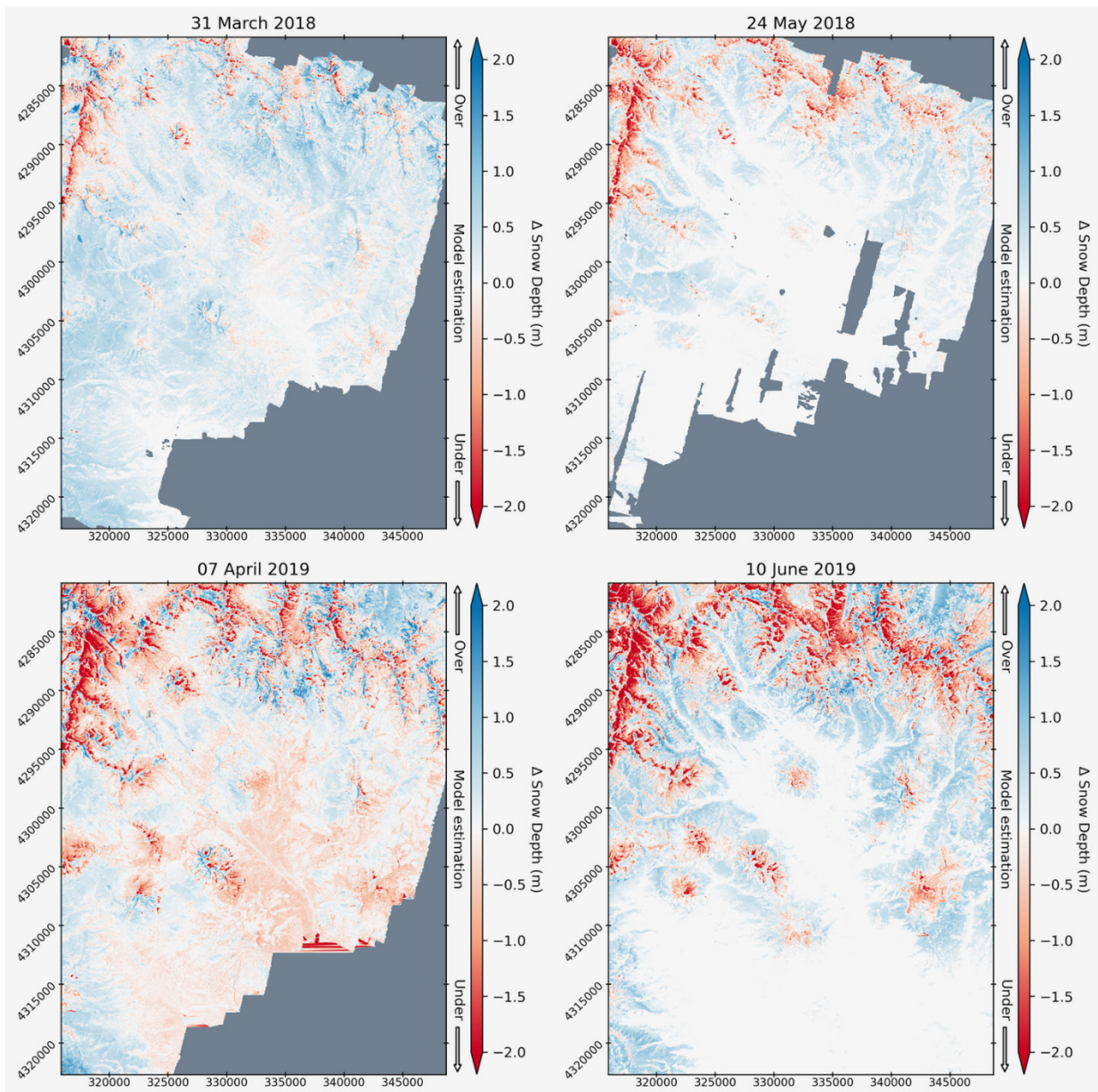
Figure 6 - Spatial comparison of simulated HRRR-iSnobal against observed ASO lidar-based snow depths for 2018 and 2019. Early season surveys (left) and the late season surveys (right) subtracted ASO values per grid cell from HRRR-iSnobal (50 m resolution).
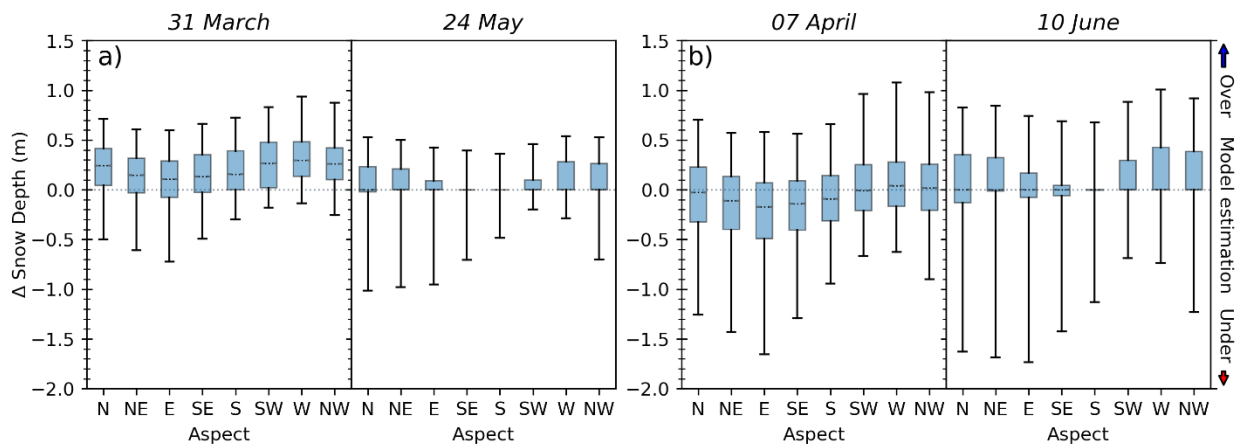

Figure 7 – Snow Depth Differences for the water years 2018 (a) and 2019 (b) between ASO and HRRR-iSnobal binned by aspect.
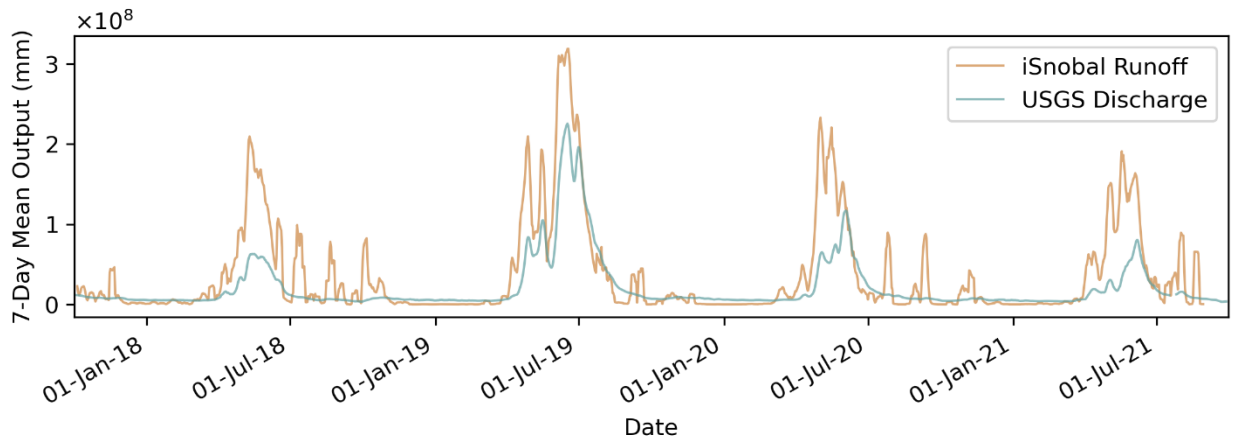
Figure 8 – Time series comparison of simulated iSnobal SWI against the measured USGS stream gauge discharge across the four water years.

5.4 Stream Gauge comparison

The watershed 7-day moving average of simulated HRRR-iSnobal SWI followed the hydrograph timing and magnitude pattern measured at the stream gauge (Figure 8). During the annual snow melt pulse, the HRRR-iSnobal SWI stayed higher relative to the measured surface water at the gauge. The time-series magnitude difference between measured discharge and simulated SWI was highest in 2018, the lowest snow year, and closest in 2019, the highest snow year. Although similar in the last days with snow depth across the SNOTEL sites in 2020 and 2021 (Table 1), the simulated SWI was different between the two years and the hydrograph had a higher peak in 2020, with a lower in 2021, following the measured stream gauge values. The later than observed simulated HRRR-iSnobal snow disappearance dates were also apparent in this comparison; a longer time lag would be expected during the receding limb of the hydrograph because the SWI is not instantaneously at the gauge. Still, the general patterns and magnitude are promising in that there is no under-forecasted SWI at any point in the melt season.

5.5 SNOW-17 comparison

Generally, precipitation used as an input to SNOW-17 was consistently higher than the HRRR precipitation input used for iSnobal across all years. The difference ranged from HRRR being 25% (2021) to 5% (2018) lower, integrated across all HRUs. A summary of the comparison, per HRU and for the full watershed, is in Table 2. Using SNOW-17 as the reference, the daily total amount difference was consistent across the HRUs and years with no high ratio differences (Supplement Figure S4). For total amounts per HRU, the poorest agreement was in the lower HRU in 2020, with HRRR 36% lower. The best agreement was found in the middle HRU in 2018, with a match of 99%. The differences per HRU were not correlated to whether it was a high or low snow year, with similar agreement in 2018 (lowest snow) and 2019 (highest snow). The poorest overall agreement (2020 and 2021) had higher precipitation amount for SNOW-17 (2020: 18%, 2021; 25%), which was not reflected in the SNOTEL site comparison. The snow depth across all sites in 2020 had a mean difference between of -0.20 m and +0.23 m and 2021 a mean difference of +0.02 m and -0.17 m in the pre-melt season (Supplement Figure S2). Both of the years had similar HRRR total precipitation amounts compared to 2018 (Differences 2020: -64 mm, 2021: -66 mm), which is also supported by the similar depth at all SNOTEL sites as 2018 (Supplemental Figure S1).

Across the four years, all three HRUs showed similar temporal patterns for daily total SWE in the snowpack although HRRR-iSnobal SWE was lower in magnitude (Figure 9) and expected following the precipitation comparison (Table 2). Consequently, he largest difference between the two models was in the upper HRU (HRRR-iSnobal between 34% to 20% lower), with less difference in the middle (HRRR-iSnobal between 20% higher and 15% lower) and lower (HRRR-iSnobal between 25% higher and 23%

Table 2 – Overview of precipitation inputs and SWE outputs for HRRR-iSnobal and SNOW-17 classified by HRU.

HRU		2018		2019		2020		2021	
		Precip.	*SWE*	*Precip.*	*SWE*	*Precip.*	*SWE*	*Precip.*	*SWE*
Lower	*HRRR-iSnobal*	300	7352	496	24976	265	12897	325	12183
	Snow-17	333	5888	566	26653	413	16816	418	13509
	Ratio	90%	125%	88%	94%	64%	77%	78%	90%
Middle	*HRRR-iSnobal*	491	30567	796	66744	471	34448	468	31574
	Snow-17	495	25375	859	67347	573	39788	606	37270
	Ratio	99%	120%	93%	99%	82%	87%	77%	85%
Upper	*HRRR-iSnobal*	667	45639	1076	107478	658	52176	599	49037
	Snow-17	707	59676	1196	135108	723	75563	832	74739
	Ratio	94%	76%	90%	80%	91%	69%	72%	66%
All	*HRRR-iSnobal*	1458	83558	2368	199198	1394	99521	1392	92794
	Snow-17	1535	90939	2621	229108	1709	132167	1856	125518
	Total	95%	92%	90%	87%	82%	75%	75%	74%

Note: Precipitation (Precip.) and SWE values are shown in mm.
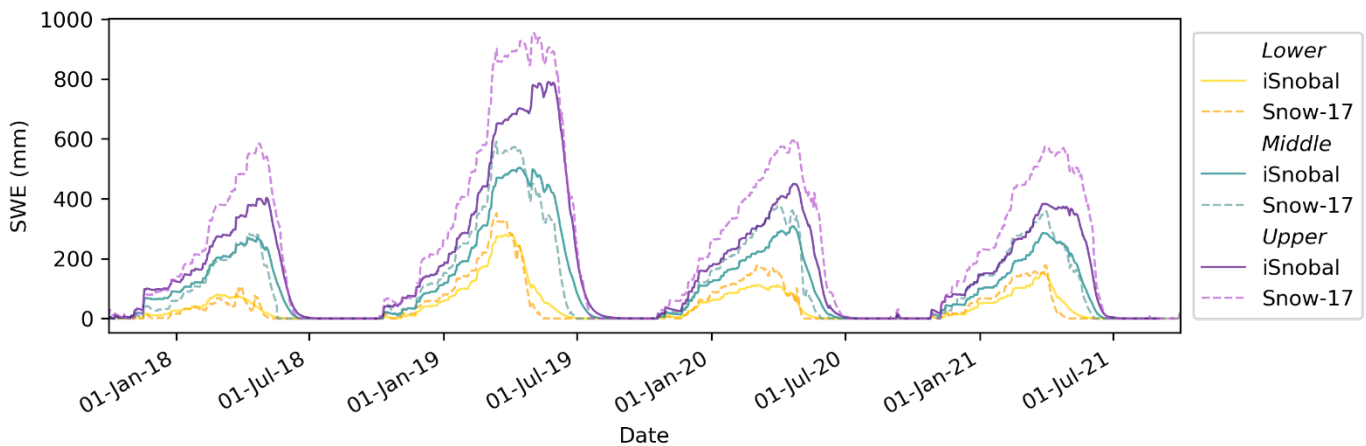

Figure 9 – Total SWE comparison per HRU across four years between SNOW-17 (dashed lines) and HRRR-iSnobal (solid lines).

lower) HRUs. As with the SNOTEL depth comparison, the basin SWE from HRRR-iSnobal showed longer persistence of snow compared to SNOW-17. This lag is most apparent in the lower and middle HRU, with the upper HRU having similar snow depletion timing.

6. Discussion

6.1 HRRR Precipitation

The results for the snow depths comparison to SNOTEL and ASO indicated that the HRRR precipitation allowed iSnobal to simulate the snow mass balance well. This is promising because HRRR data are distributed at 3 km resolution and are much coarser than the 50 m model output resolution, which is needed to resolve the different physical processes influencing the snowpack evolution in this type of terrain (Winstral et al., 2014). The difference in resolutions makes it challenging to properly adjust for the topographic precipitation differences, especially with the model domain's high vertical relief (1420 m). Kilometer scale NWP model resolutions are known to underestimate snowfall at higher elevations, and complex terrain is particularly challenging to simulate snowpack evolution with inconsistent snowfall trends (Ikeda 2010). The current solutions to 'bias correct' and improve

345   NWP precipitation based on topography are basin and application specific. For example, Bellaire et al. (2011, 2013) applied a constant correction factor and Griessinger et al. (2019) corrected and filtered with observations from a dense in-situ network. These approaches require in-situ observation and basin-specific knowledge that is not always available, reducing transferability to other regions. Ultimately, the fewer corrections needed to forcing inputs results in greater potential to scale and adapt model setups into forecast operations. The presented workflow here had no changes to the HRRR inputs and precipitation was used 'as is'.

350   Given the different methods to determine precipitation in HRRR and as inputs to SNOW-17, a match between the two was not expected. The calibration process for SNOW-17 precipitation inputs uses spatially sparse in-situ point measurements and empirical data from previous water years. As an atmospheric model, HRRR is a product of assimilated observation, physically based modeling, and a fundamentally different approach. Neither set of precipitation values were considered the truth, and accurately measuring precipitation is an unsolved challenge in mountain terrain. Additional work is needed to understand the variation in

355   HRRR values relative to the calibrated precipitation used by the CBRFC across these water years (i.e poorer agreement in 2020 and 2021).

6.2 Comparison Data Sources

    The snow depth comparison of this work used in-situ point observations and aerial spatial measurements. Both sources had no consistent agreement, with the spatial measurements tending to be lower than the point data. This underestimation has been shown

360   to exist when comparing point data to spatial averages of snow depth from lidar (Trujillo and Lehning, 2015). Similarly, in-situ snow depth estimates from point observation stations, such as SNOTEL, are known to only represent a small surrounding footprint because of the large heterogeneity of snow depth in alpine environments (Molotch and Bales, 2005). This limitation, in part, can explain the higher spread of the iSnobal snow depths to the SNOTEL stations, as the values represent a larger area around them (Figure 3). The strength of SNOTEL station data is as long-term historical records, from which index methods could be developed

365   and help understand changes over long timeframes (Harpold et al., 2012; Musselman et al., 2021; Trujillo and Molotch, 2014). In the case of this work, it was the only source available to allow a model performance assessment over multiple years. The results from the SNOTEL comparison gave confidence that the HRRR forcing inputs provided a quality long-term input source, in terms of capturing peak snow depth, for a watershed with only sparse in-situ meteorological observations across different snow seasons. The addition of aerial observations, such as ASO, has improved the ability to retrieve snow depth over large areas and supplies

370   valuable validation data used in many studies (Brandt et al., 2020; Hedrick et al., 2018; McGrath et al., 2019). In this work, the ASO maps enabled a spatial comparison that was impossible in the past. The comparison identified differences in snow depth at high elevations and across aspects that are not possible with SNOTEL stations, which are generally located in relatively flat middle and lower elevations (e.g., below 3261 m in ERW). Additionally, the snow depth disagreements between measured ASO and SNOTEL highlighted that SNOTEL observations could not represent snow conditions at 50 m model output resolutions either, and

375   caution is urged when using SNOTEL snow depth data as 'truth' for spatially distributed models. Likewise, the inconsistent comparison results to SNOTEL showed that coarser aerial product resolutions should also not be treated as truth, and snow depths can vary within short distances due to the high spatial variability of mountain terrain.

6.3 Physically Based Models

    Accurately simulating the seasonal snow accumulation and depletion across multiple years and different topographic regions

380   through a single model is still an unsolved challenge. However, physically based models are better suited to fulfill this need when compared to temperature index-based models. Existing studies using long-term records of SNOTEL measurements have identified a need for physically based modeling approaches as they can better show the impacts on water supply from current and projected

14

climatological changes (Harpold et al., 2012; Musselman et al., 2021; Trujillo and Molotch, 2014). Physically based models are capable of accounting for scenarios such as shifting snowmelt rates (Musselman et al., 2017), changes to the length of snow accumulation and melt season (Trujillo and Molotch, 2014), accelerated melt due to darker snow (Skiles et al., 2018), and rain on snow events (Marks et al., 1998).

The HRRR-iSnobal combination in this work closely simulated the snow depth observations from one region across different seasonal characteristics (average vs. non-average year) without a-priori region-specific knowledge. All required forcing data per water year only used the HRRR forecasted observations of that year, replacing the sparse in-situ measurements that are interpolated and calibrated with historical data. The interpolation and calibration procedures are essential steps in the current Snow-17 workflow of the CBRFC and require regional forecaster experience. Voiding this need gives a major operational advantage by simplifying model application and enhancing the ability to adapt to environmental changes across different regions and water years.

In addition to the streamlined forcing data preparation, the advantages during the water year simulation include the replacement of region-specific parameters required by temperature index models (e.g., the Snow-17 melt factor) with the energy balance calculations from physically based models. The index model parameters depend again on forecaster experience and require forecaster changes in response to changing environmental conditions (average vs. non-average). In this work, there was no need to change the model configuration between the 2018 (average) and the 2019 (above-average) years in HRRR-iSnobal. The seasonal differences were accounted for explicitly as the snow energy balance calculations includes influences such as shortwave radiation (Marks and Dozier, 1992), longwave radiation (Link and Marks, 1999), and turbulent fluxes from terrain-dependent wind speeds (Winstral and Marks, 2002).

Lastly, iSnobal is a spatially distributed model run with a user-defined pixel size (50 m in this study) and set up with site-specific elevation and vegetation data information from the model domain. This configuration negated the need to divide the model domain into uniform and simplified HRUs to simulate the topographic differences of the model domain accurately. In summary, physically based models remove the dependence on long-term historical data, reduce the need for model application knowledge, and better account for physiographic factors, which result in improved scalability across different seasonal and terrain-dependent snowpack dynamics. Gradually adding these models into operational settings, with architectures presented in this work, can provide snowpack response information with current environmental perturbations. Their addition will enhance the quality and expand the ability to adapt to current and future water supply forecast needs.

6.4 Improvements to iSnobal

The consistent longer presence of snow in HRRR-iSnobal relative to the observations across the simulated years highlighted an area for improvement. One cause for the delay is attributed to the too low amount of calculated shortwave radiation by SMRF, not providing enough energy to drive snowmelt in iSnobal. An obvious option that influences the calculation is the snow albedo time-decay function, which has caused high uncertainty in many different model types and scales (Chen et al., 2014; Clark et al., 2015; Krinner et al., 2018; Qu and Hall, 2014; Ryken et al., 2020). The decay function determines the snow albedo based on the time of the last snowfall when the albedo gets reset, and the decay starts anew. A drawback of this approach is excluding other events that change the albedo, such as dust deposition. Solutions for the 1-d Snobal model improved the simulated snowmelt timing and forced the model with observed snow albedo (Miller et al., 2016; Skiles and Painter, 2019; Skiles et al., 2015, 2012). Scaling this solution and adapting it into spatially distributed models requires data sources with daily updated and spatially complete snow albedo, which are available today from remote sensing observations. For instance, the combined Moderate-Resolution Imaging Spectroradiometer (MODIS) Snow Covered Area and Grain Size (MODSCAG) and Dust Radiative Forcing (MODDRFS) in Snow (Rittger et al., 2020) provides daily observation with 500 m spatial resolution. This spatial and temporal resolution fulfills the
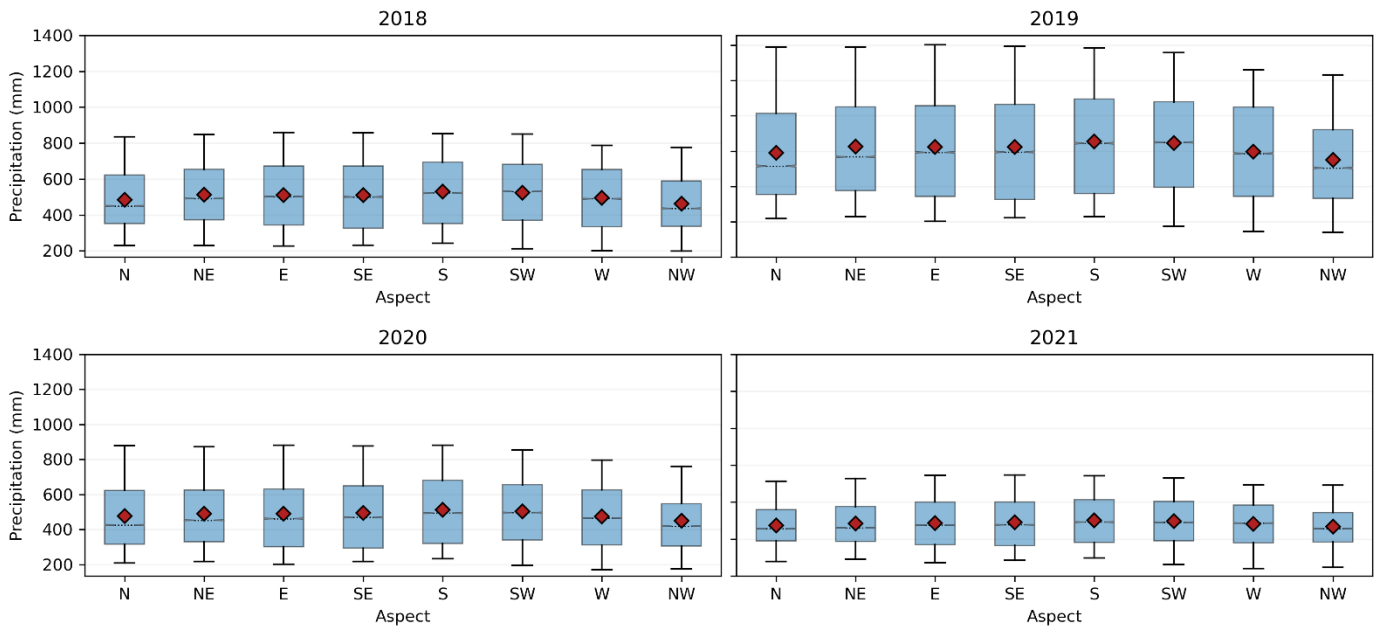
Figure 10 – Comparison of the SMRF distributed total annual HRRR precipitation amounts per pixel categorized by aspect across the years. Mean values are shown with the red diamond, while the dashed lines are the median values.

requirements of a model data source. With the demonstrated need for improved snow disappearance dates of this work, improved results by using observations in other work, and the availability of remote sensing products, we suggest integrating remotely sensed snow albedo into iSnobal.

425   Though relatively sparse in time, the spatial snow depth comparison results highlighted another area to target with HRRR-iSnobal. The snow depths differences by aspect (Figures 5c and 5d) indicated an iSnobal energy balance issue as there was no strong aspect bias coming from the HRRR precipitation data (Figure 10). This difference could also be caused by the disabled feature to account for wind-redistribution. However, the closer agreements on the south-facing aspect, especially in the late season ASO surveys, suggest that improving the incoming shortwave radiation could help address this model bias. Shortwave radiation is currently a

430   topographically adjusted calculation (Dozier 1990) by SMRF when preparing iSnobal forcing inputs. One alternative to this approach is to use the supplied values by HRRR, reducing model complexity and computation times. The addition of remotely sensed albedo and alternative handling for incoming shortwave radiation will be the follow-up effort for iSnobal to this work.

7 Conclusions

This work presented and evaluated the spatially distributed iSnobal model forced with HRRR meteorological data to expand the

435   model options and support operational water forecasts for the CBRFC. The model was assessed over one representative headwater basin in the CRB with an area of 1373 km^2 for four consecutive water years (2018 - 2021) at a 50 m spatial resolution and hourly time steps. There were several key outcomes from this effort: (1) Execution times from one to the next day and total storage requirements would allow operational forecasters to run HRRR-iSnobal alongside current production environments (2) HRRR provided meteorological input data that enabled iSnobal to simulate close to the observed snow depths up to peak accumulation

440   (3) iSnobal radiation calculations need revisions to improve melt timing and to address geographic aspect bias (4) Simulated timing and magnitude of iSnobal SWI followed the observed hydrograph at the basin stream gauge.

From the model comparison, the iSnobal SWE was lower than the SNOW-17 SWE and consistent with the lower precipitation inputs from HRRR than the SNOW-17 inputs. iSnobal had lower snow depths at higher elevations relative to aerial observations and was attributed to the coarser model output resolution of HRRR relative to the topography and the simulated spatial resolution.

Model runs in additional basins are ongoing and will allow further evaluation if this is consistent. Despite these differences, iSnobal simulated snow depths close to measured values across the watershed up to the melt period. Once snowmelt set in, iSnobal snow depths showed greater disagreement than the observed in-situ measurement sites and simulated longer snow persistence. The discrepancy between observed and simulated snowmelt timing, and therefore magnitude, was consistent across the years, including above-average and below-average snow years. Accurately simulating snow depletion timing is important for operational adoption.

Future work to address snowmelt timing aims to improve snow energy balance calculations, specifically by using remotely observed snow albedo data and updating the net shortwave radiation treatment in iSnobal. Nevertheless, as the world transitions into a future that is less similar to the past and statistical models become less reliable, this work showed that HRRR-iSnobal could be a valuable supplement to operational water supply forecasting methods in snow-dominated regions.

Code availability

The software components used to run the model and analyze the results are publicly available. iSnobal model components are available via the USDA ARS NWRC GitHub page: https://github.com/USDA-ARS-NWRC. For this study, GitHub forks for SMRF (https://doi.org/10.5281/zenodo.6543935), AWSM (https://doi.org/10.5281/zenodo.6543919), and weather forecast retrieval (https://doi.org/10.5281/zenodo.6543579) were created to capture the model code at the time of completing this study as no official version was released. The forks can be found under https://github.com/UofU-Cryosphere. Additions to model setup and result analysis code are stored on https://github.com/UofU-Cryosphere/isnoda (https://doi.org/10.5281/zenodo.6543995).

Data availability

The following datasets were used for the model runs and comparisons:

- The National Elevation Dataset (NED), U.S. Department of the Interior, Geological Survey https://apps.nationalmap.gov/viewer/, last access: 28 February 2022.
- LANDFIRE, 2014, Existing Vegetation Type and Height Layer, LANDFIRE 1.4.0, U.S. Department of the Interior, Geological Survey, and U.S. Department of AgricultureData Product Mosaic Downloads: https://landfire.gov/getdata.php, last access: 28 February 2022.
- NOAA The High-Resolution Rapid Refresh (HRRR): https://rapidrefresh.noaa.gov/hrrr/, last access: 28 February 2022.
- NRCS National Water and Climate Center | SNOTEL | SWE Data: https://www.wcc.nrcs.usda.gov/snow/SNOTEL-wedata.html, last access: 28 February 2022.
- The National Map | U.S. Geological Survey: https://www.usgs.gov/programs/national-geospatial-program/national-map, last access: 28 February 2022.
- USGS Surface Water data for USA: USGS Surface-Water Daily Statistics: https://waterdata.usgs.gov/nwis/dvstat/?site_no=09112500&referred_module=sw&format=sites_selection_links, last access: 28 February 2022.
- Painter, T. H.: ASO L4 Lidar Snow Depth 50m UTM Grid, Version 1. [USCOGE]. Boulder, Colorado USA. NASA National Snow and Ice Data Center Distributed Active Archive Center, NSIDC, https://doi.org/10.5067/STOT5I0U1WVI, 2018.

References

Anderson, E. A.: A point energy and mass balance model of a snow cover, 1976.

Automated Water Supply Model — awsm documentation: https://awsm.readthedocs.io/en/latest/readme.html, last access: 28 February 2022.

Spatial Modeling for Resources Framework — SMRF documentation: https://smrf.readthedocs.io/en/latest/, last access: 28 February 2022.

Ayers, J., Ficklin, D. L., Stewart, I. T., and Strunk, M.: Comparison of CMIP3 and CMIP5 projected hydrologic conditions over the Upper Colorado River Basin, International Journal of Climatology, 36, 3807–3818, https://doi.org/10.1002/joc.4594, 2016.

Bellaire, S., Jamieson, J. B., and Fierz, C.: Forcing the snow-cover model SNOWPACK with forecasted weather data, The Cryosphere, 5, 1115–1125, https://doi.org/10.5194/tc-5-1115-2011, 2011.

Bellaire, S., Jamieson, J. B., and Fierz, C.: Corrigendum to "Forcing the snow-cover model SNOWPACK with forecasted weather data" published in The Cryosphere, 5, 1115–1125, 2011, The Cryosphere, 7, 511–513, https://doi.org/10.5194/tc-7-511-2013, 2013.

Benjamin, S. G., Weygandt, S. S., Brown, J. M., Hu, M., Alexander, C. R., Smirnova, T. G., Olson, J. B., James, E. P., Dowell, D. C., Grell, G. A., Lin, H., Peckham, S. E., Smith, T. L., Moninger, W. R., Kenyon, J. S., and Manikin, G. S.: A North American Hourly Assimilation and Model Forecast Cycle: The Rapid Refresh, Monthly Weather Review, 144, 1669–1694, https://doi.org/10.1175/MWR-D-15-0242.1, 2016.

Brandt, W. T., Bormann, K. J., Cannon, F., Deems, J. S., Painter, T. H., Steinhoff, D. F., and Dozier, J.: Quantifying the Spatial Variability of a Snowstorm Using Differential Airborne Lidar, Water Resour. Res., 56, https://doi.org/10.1029/2019WR025331, 2020.

510   Bryant, A. C., Painter, T. H., Deems, J. S., and Bender, S. M.: Impact of dust radiative forcing in snow on accuracy of operational runoff prediction in the Upper Colorado River Basin: DUST IN SNOW IMPACT ON STREAMFLOW, Geophys. Res. Lett., 40, 3945–3949, https://doi.org/10.1002/grl.50773, 2013.

Bytheway, J. L., Kummerow, C. D., and Alexander, C.: A Features-Based Assessment of the Evolution of Warm Season Precipitation Forecasts from the HRRR Model over Three Years of Development, Weather and Forecasting, 32, 1841–1856,
515   https://doi.org/10.1175/WAF-D-17-0050.1, 2017.

Chen, F., Barlage, M., Tewari, M., Rasmussen, R., Jin, J., Lettenmaier, D., Livneh, B., Lin, C., Miguez-Macho, G., Niu, G.-Y., Wen, L., and Yang, Z.-L.: Modeling seasonal snowpack evolution in the complex terrain and forested Colorado Headwaters region: A model intercomparison study, J. Geophys. Res. Atmos., 119, 13,795-13,819, https://doi.org/10.1002/2014JD022167, 2014.

Cho, E., McCrary, R. R., and Jacobs, J. M.: Future Changes in Snowpack, Snowmelt, and Runoff Potential Extremes Over North
520   America, Geophysical Research Letters, 48, e2021GL094985, https://doi.org/10.1029/2021GL094985, 2021.

Christensen, N. S. and Lettenmaier, D. P.: A multimodel ensemble approach to assessment of climate change impacts on the hydrology and water resources of the Colorado River Basin, Hydrology and Earth System Sciences, 11, 1417–1434, https://doi.org/10.5194/hess-11-1417-2007, 2007.

Clark, M. P., Nijssen, B., Lundquist, J. D., Kavetski, D., Rupp, D. E., Woods, R. A., Freer, J. E., Gutmann, E. D., Wood, A. W.,
525   Gochis, D. J., Rasmussen, R. M., Tarboton, D. G., Mahat, V., Flerchinger, G. N., and Marks, D. G.: A unified approach for process-based hydrologic modeling: 2. Model implementation and case studies, Water Resources Research, 51, 2515–2542, https://doi.org/10.1002/2015WR017200, 2015.

Council, N. R.: Toward a new advanced hydrologic prediction service (AHPS), The National Academies Press, Washington, DC, 84 pp., https://doi.org/10.17226/11598, 2006.

530   Dettinger, M., Udall, B., and Georgakakos, A.: Western water and climate change, Ecological Applications, 25, 2069–2093, https://doi.org/10.1890/15-0938.1, 2015.

Dozier, J. and Frew, J.: Rapid calculation of terrain parameters for radiation modeling from digital elevation data, IEEE Transactions on Geoscience and Remote Sensing, 28, 963–969, https://doi.org/10.1109/36.58986, 1990.

Essery, R.: A factorial snowpack model (FSM 1.0), Geosci. Model Dev., 8, 3867–3876, https://doi.org/10.5194/gmd-8-3867-2015,
535   2015.

Feng, S. and Hu, Q.: Changes in winter snowfall/precipitation ratio in the contiguous United States, Journal of Geophysical Research: Atmospheres, 112, https://doi.org/10.1029/2007JD008397, 2007.

Forthofer, J. M., Butler, B. W., Wagenbrenner, N. S., Forthofer, J. M., Butler, B. W., and Wagenbrenner, N. S.: A comparison of three approaches for simulating fine-scale surface winds in support of wildland fire management. Part I. Model formulation and
540   comparison against measurements, Int. J. Wildland Fire, 23, 969–981, https://doi.org/10.1071/WF12089, 2014.

Franz, K. J., Hogue, T. S., and Sorooshian, S.: Operational snow modeling: Addressing the challenges of an energy balance model for National Weather Service forecasts, Journal of Hydrology, 360, 48–66, https://doi.org/10.1016/j.jhydrol.2008.07.013, 2008.

Franz, K. J., Butcher, P., and Ajami, N. K.: Addressing snow model uncertainty for hydrologic prediction, Advances in Water Resources, 33, 820–832, https://doi.org/10.1016/j.advwatres.2010.05.004, 2010.

545   Garen, D. C. and Marks, D.: Spatially distributed energy balance snowmelt modelling in a mountainous river basin: estimation of meteorological inputs and verification of model results, Journal of Hydrology, 315, 126–153, https://doi.org/10.1016/j.jhydrol.2005.03.026, 2005.

Gowan, T. A., Horel, J. D., Jacques, A. A., and Kovac, A.: Using Cloud Computing to Analyze Model Output Archived in Zarr Format, Journal of Atmospheric and Oceanic Technology, 1, https://doi.org/10.1175/JTECH-D-21-0106.1, 2022.

550 Griessinger, N., Schirmer, M., Helbig, N., Winstral, A., Michel, A., and Jonas, T.: Implications of observation-enhanced energy-balance snowmelt simulations for runoff modeling of Alpine catchments, Advances in Water Resources, 133, 103410, https://doi.org/10.1016/j.advwatres.2019.103410, 2019.

Harpold, A., Brooks, P., Rajagopal, S., Heidbuchel, I., Jardine, A., and Stielstra, C.: Changes in snowpack accumulation and ablation in the intermountain west, Water Resources Research, 48, https://doi.org/10.1029/2012WR011949, 2012.

555 Havens, S., Marks, D., Kormos, P., and Hedrick, A.: Spatial Modeling for Resources Framework (SMRF): A modular framework for developing spatial forcing data for snow modeling in mountain basins, Computers & Geosciences, 109, 295–304, https://doi.org/10.1016/j.cageo.2017.08.016, 2017.

Havens, S., Marks, D., FitzGerald, K., Masarik, M., Flores, A. N., Kormos, P., and Hedrick, A.: Approximating Input Data to a Snowmelt Model Using Weather Research and Forecasting Model Outputs in Lieu of Meteorological Measurements, Journal of
560 Hydrometeorology, 20, 847–862, https://doi.org/10.1175/JHM-D-18-0146.1, 2019.

Havens, S., Marks, D., Sandusky, M., Hedrick, A., Johnson, M., Robertson, M., and Trujillo, E.: Automated Water Supply Model (AWSM): Streamlining and standardizing application of a physically based snow model for water resources and reproducible science, Computers & Geosciences, 144, 104571, https://doi.org/10.1016/j.cageo.2020.104571, 2020.

He, M., Hogue, T. S., Franz, K. J., Margulis, S. A., and Vrugt, J. A.: Characterizing parameter sensitivity and uncertainty for a
565 snow model across hydroclimatic regimes, Advances in Water Resources, 34, 114–127, https://doi.org/10.1016/j.advwatres.2010.10.002, 2011.

Hedrick, A. R., Marks, D., Havens, S., Robertson, M., Johnson, M., Sandusky, M., Marshall, H., Kormos, P. R., Bormann, K. J., and Painter, T. H.: Direct Insertion of NASA Airborne Snow Observatory-Derived Snow Depth Time Series Into the iSnobal Energy Balance Snow Model, Water Resour. Res., 54, 8045–8063, https://doi.org/10.1029/2018WR023190, 2018.

570 Hedrick, A. R., Marks, D., Marshall, H., McNamara, J., Havens, S., Trujillo, E., Sandusky, M., Robertson, M., Johnson, M., Bormann, K. J., and Painter, T. H.: From Drought to Flood: A Water Balance Analysis of the Tuolumne River Basin during Extreme Conditions (2015 – 2017), Hydrological Processes, hyp.13749, https://doi.org/10.1002/hyp.13749, 2020.

Hubbard, S. S., Williams, K. H., Agarwal, D., Banfield, J., Beller, H., Bouskill, N., Brodie, E., Carroll, R., Dafflon, B., Dwivedi, D., Falco, N., Faybishenko, B., Maxwell, R., Nico, P., Steefel, C., Steltzer, H., Tokunaga, T., Tran, P. A., Wainwright, H., and
575 Varadharajan, C.: The East River, Colorado, Watershed: A Mountainous Community Testbed for Improving Predictive Understanding of Multiscale Hydrological–Biogeochemical Dynamics, Vadose Zone Journal, 17, 0, https://doi.org/10.2136/vzj2018.03.0061, 2018.

Ikeda, K., Rasmussen, R., Liu, C., Newman, A., Chen, F., Barlage, M., Gutmann, E., Dudhia, J., Dai, A., Luce, C., and Musselman, K.: Snowfall and snowpack in the Western U.S. as captured by convection permitting climate simulations: current climate and
580 pseudo global warming future climate, Clim Dyn, 57, 2191–2215, https://doi.org/10.1007/s00382-021-05805-w, 2021.

Iwamoto, K., Yamaguchi, S., Nakai, S., and Sato, A.: Forecasting Experiments Using the Regional Meteorological Model and the Numerical Snow Cover Model in the Snow Disaster Forecasting System, Journal of Natural Disaster Science, 30, 35–43, https://doi.org/10.2328/jnds.30.35, 2008.

Knowles, N., Dettinger, M. D., and Cayan, D. R.: Trends in Snowfall versus Rainfall in the Western United States, Journal of
585 Climate, 19, 4545–4559, https://doi.org/10.1175/JCLI3850.1, 2006.

Kormos, P. R., Marks, D., McNamara, J. P., Marshall, H. P., Winstral, A., and Flores, A. N.: Snow distribution, melt and surface water inputs to the soil in the mountain rain–snow transition zone, Journal of Hydrology, 519, 190–204, https://doi.org/10.1016/j.jhydrol.2014.06.051, 2014.

Krinner, G., Derksen, C., Essery, R., Flanner, M., Hagemann, S., Clark, M., Hall, A., Rott, H., Brutel-Vuilmet, C., Kim, H.,
Ménard, C. B., Mudryk, L., Thackeray, C., Wang, L., Arduini, G., Balsamo, G., Bartlett, P., Boike, J., Boone, A., Chéruy, F.,
Colin, J., Cuntz, M., Dai, Y., Decharme, B., Derry, J., Ducharne, A., Dutra, E., Fang, X., Fierz, C., Ghattas, J., Gusev, Y., Haverd,
V., Kontu, A., Lafaysse, M., Law, R., Lawrence, D., Li, W., Marke, T., Marks, D., Ménégoz, M., Nasonova, O., Nitta, T., Niwano,
M., Pomeroy, J., Raleigh, M. S., Schaedler, G., Semenov, V., Smirnova, T. G., Stacke, T., Strasser, U., Svenson, S., Turkov, D.,
Wang, T., Wever, N., Yuan, H., Zhou, W., and Zhu, D.: ESM-SnowMIP: assessing snow models and quantifying snow-related
climate feedbacks, Geoscientific Model Development, 11, 5027–5049, https://doi.org/10.5194/gmd-11-5027-2018, 2018.

Lehning, M., Bartelt, P., Brown, B., Fierz, C., and Satyawali, P.: A physical SNOWPACK model for the Swiss avalanche warning:
Part II. Snow microstructure, Cold Regions Science and Technology, 35, 147–167, https://doi.org/10.1016/S0165-232X(02)00073-
3, 2002.

Li, D., Wrzesien, M. L., Durand, M., Adam, J., and Lettenmaier, D. P.: How much runoff originates as snow in the western United
States, and how will that change in the future?, Geophys. Res. Lett., 44, 6163–6172, https://doi.org/10.1002/2017GL073551, 2017.

Link, T. and Marks, D.: Distributed simulation of snowcover mass- and energy-balance in the boreal forest, Hydrol. Process., 13,
2439–2452, https://doi.org/10.1002/(SICI)1099-1085(199910)13:14/15<2439::AID-HYP866>3.0.CO;2-1, 1999.

Liston, G. E. and Elder, K.: A Distributed Snow-Evolution Modeling System (SnowModel), Journal of Hydrometeorology, 7,
1259–1276, https://doi.org/10.1175/JHM548.1, 2006.

Marks, D. and Dozier, J.: Climate and energy exchange at the snow surface in the Alpine Region of the Sierra Nevada: 2. Snow
cover energy balance, Water Resources Research, 28, 3043–3054, https://doi.org/10.1029/92WR01483, 1992.

Marks, D., Dozier, J., and Davis, R. E.: Climate and energy exchange at the snow surface in the Alpine Region of the Sierra
Nevada: 1. Meteorological measurements and monitoring, Water Resources Research, 28, 3029–3042,
https://doi.org/10.1029/92WR01482, 1992.

Marks, D., Kimball, J., Tingey, D., and Link, T.: The sensitivity of snowmelt processes to climate conditions and forest cover
during rain-on-snow: a case study of the 1996 Pacific Northwest flood, Hydrol. Process., 12, 1569–1587,
https://doi.org/10.1002/(SICI)1099-1085(199808/09)12:10/11<1569::AID-HYP682>3.0.CO;2-L, 1998.

Marks, D., Domingo, J., Susong, D., Link, T., and Garen, D.: A spatially distributed energy balance snowmelt model for application
in mountain basins, HYDROLOGICAL PROCESSES, 13, 26, 1999.

McGrath, D., Webb, R., Shean, D., Bonnell, R., Marshall, H.-P., Painter, T. H., Molotch, N. P., Elder, K., Hiemstra, C., and
Brucker, L.: Spatially Extensive Ground-Penetrating Radar Snow Depth Observations During NASA's 2017 SnowEx Campaign:
Comparison With In Situ, Airborne, and Satellite Observations, Water Resour. Res., 55, 10026–10036,
https://doi.org/10.1029/2019WR024907, 2019.

Miller, S. D., Wang, F., Burgess, A. B., Skiles, S. M., Rogers, M., and Painter, T. H.: Satellite-Based Estimation of Temporally
Resolved Dust Radiative Forcing in Snow Cover, Journal of Hydrometeorology, 17, 1999–2011, https://doi.org/10.1175/JHM-D-
15-0150.1, 2016.

Molotch, N. P. and Bales, R. C.: Scaling snow observations from the point to the grid element: Implications for observation network
design, Water Resour. Res., 41, https://doi.org/10.1029/2005WR004229, 2005.

Mote, P. W., Li, S., Lettenmaier, D. P., Xiao, M., and Engel, R.: Dramatic declines in snowpack in the western US, npj Climate
and Atmospheric Science, 1, 2, https://doi.org/10.1038/s41612-018-0012-1, 2018.

Musselman, K. N., Clark, M. P., Liu, C., Ikeda, K., and Rasmussen, R.: Slower snowmelt in a warmer world, Nature Clim Change,
7, 214–219, https://doi.org/10.1038/nclimate3225, 2017.

Musselman, K. N., Addor, N., Vano, J. A., and Molotch, N. P.: Winter melt trends portend widespread declines in snow water resources, Nat. Clim. Chang., 11, 418–424, https://doi.org/10.1038/s41558-021-01014-9, 2021.

630 Painter, T. H., Berisford, D. F., Boardman, J. W., Bormann, K. J., Deems, J. S., Gehrke, F., Hedrick, A., Joyce, M., Laidlaw, R., Marks, D., Mattmann, C., McGurk, B., Ramirez, P., Richardson, M., Skiles, S. M., Seidel, F. C., and Winstral, A.: The Airborne Snow Observatory: Fusion of scanning lidar, imaging spectrometer, and physically-based modeling for mapping snow water equivalent and snow albedo, Remote Sensing of Environment, 184, 139–152, https://doi.org/10.1016/j.rse.2016.06.018, 2016.

Painter, T. H., Skiles, S. M., Deems, J. S., Brandt, W. T., and Dozier, J.: Variation in Rising Limb of Colorado River Snowmelt
635 Runoff Hydrograph Controlled by Dust Radiative Forcing in Snow, Geophysical Research Letters, https://doi.org/10.1002/2017GL075826, 2018.

Qu, X. and Hall, A.: On the persistent spread in snow-albedo feedback, Clim Dyn, 42, 69–81, https://doi.org/10.1007/s00382-013-1774-0, 2014.

Rittger, K., Raleigh, M. S., Dozier, J., Hill, A. F., Lutz, J. A., and Painter, T. H.: Canopy Adjustment and Improved Cloud Detection
640 for Remotely Sensed Snow Cover Mapping, Water Resources Research, 56, e2019WR024914, https://doi.org/10.1029/2019WR024914, 2020.

Ryken, A., Bearup, L. A., Jefferson, J. L., Constantine, P., and Maxwell, R. M.: Sensitivity and model reduction of simulated snow processes: Contrasting observational and parameter uncertainty to improve prediction, Advances in Water Resources, 135, 103473, https://doi.org/10.1016/j.advwatres.2019.103473, 2020.

645 Schirmer, M. and Jamieson, B.: Verification of analysed and forecasted winter precipitation in complex terrain, The Cryosphere, 9, 587–601, https://doi.org/10.5194/tc-9-587-2015, 2015.

Schmucki, E., Marty, C., Fierz, C., and Lehning, M.: Evaluation of modelled snow depth and snow water equivalent at three contrasting sites in Switzerland using SNOWPACK simulations driven by different meteorological data input, Cold Regions Science and Technology, 99, 27–37, https://doi.org/10.1016/j.coldregions.2013.12.004, 2014.

650 Skiles, S. M. and Painter, T.: Daily evolution in dust and black carbon content, snow grain size, and snow albedo during snowmelt, Rocky Mountains, Colorado, Journal of Glaciology, 63, 118–132, https://doi.org/10.1017/jog.2016.125, 2017.

Skiles, S. M. and Painter, T. H.: Toward Understanding Direct Absorption and Grain Size Feedbacks by Dust Radiative Forcing in Snow With Coupled Snow Physical and Radiative Transfer Modeling, Water Resour. Res., 55, 7362–7378, https://doi.org/10.1029/2018WR024573, 2019.

655 Skiles, S. M., Painter, T. H., Deems, J. S., Bryant, A. C., and Landry, C. C.: Dust radiative forcing in snow of the Upper Colorado River Basin: 2. Interannual variability in radiative forcing and snowmelt rates, Water Resources Research, 48, https://doi.org/10.1029/2012WR011986, 2012.

Skiles, S. M., Painter, T. H., Belnap, J., Holland, L., Reynolds, R. L., Goldstein, H. L., and Lin, J.: Regional variability in dust-on-snow processes and impacts in the Upper Colorado River Basin, Hydrological Processes, 29, 5397–5413,
660 https://doi.org/10.1002/hyp.10569, 2015.

Slater, A. G., Barrett, A. P., Clark, M. P., Lundquist, J. D., and Raleigh, M. S.: Uncertainty in seasonal snow reconstruction: Relative impacts of model forcing and image availability, Advances in Water Resources, 55, 165–177, https://doi.org/10.1016/j.advwatres.2012.07.006, 2013.

Stewart, I. T.: Changes in snowpack and snowmelt runoff for key mountain regions, Hydrological Processes, 23, 78–94,
665 https://doi.org/10.1002/hyp.7128, 2009.

The Bureau of Reclamation: Emerging Technologies in Snow, 2022.

Trujillo, E. and Lehning, M.: Theoretical analysis of errors when estimating snow distribution through point measurements, The Cryosphere, 9, 1249–1264, https://doi.org/10.5194/tc-9-1249-2015, 2015.

Trujillo, E. and Molotch, N. P.: Snowpack regimes of the Western United States, Water Resources Research, 50, 5611–5623, https://doi.org/10.1002/2013WR014753, 2014.

Vernay, M., Lafaysse, M., Monteiro, D., Hagenmuller, P., Nheili, R., Samacoïts, R., Verfaillie, D., and Morin, S.: The S2M meteorological and snow cover reanalysis over the French mountainous areas, description and evaluation (1958–2020), Earth System Science Data Discussions, 1–36, https://doi.org/10.5194/essd-2021-249, 2021.

Vionnet, V., Brun, E., Morin, S., Boone, A., Faroux, S., Le Moigne, P., Martin, E., and Willemet, J.-M.: The detailed snowpack scheme Crocus and its implementation in SURFEX v7.2, Geoscientific Model Development, 5, 773–791, https://doi.org/10.5194/gmd-5-773-2012, 2012.

Winstral, A. and Marks, D.: Simulating wind fields and snow redistribution using terrain-based parameters to model snow accumulation and melt over a semi-arid mountain catchment, Hydrological Processes, 16, 3585–3603, https://doi.org/10.1002/hyp.1238, 2002.

Winstral, A., Marks, D., and Gurney, R.: Assessing the Sensitivities of a Distributed Snow Model to Forcing Data Resolution, Journal of Hydrometeorology, 15, 1366–1383, https://doi.org/10.1175/JHM-D-13-0169.1, 2014.